# Cu(In,Ga)$S_2$ THIN-FILM SOLAR CELLS PREPARED BY $H_2S$ SULFURIZATION OF CuGa-In PRECURSOR[1]

Neelkanth G. Dhere, Shashank R. Kulkarni, Sanjay S. Chavan and Shantinath R. Ghongadi
Florida Solar Energy Center
Cocoa, FL 32922-5703

ABSTRATCT

Thin-film $CuInS_2$ solar cell is the leading candidate for space power because of bandgap near the optimum value for AM0 solar radiation outside the earth's atmosphere, excellent radiation hardness, and freedom from intrinsic degradation mechanisms unlike a-Si:H cells. Ultra-lightweight thin-film solar cells deposited on flexible polyimide plastic substrates such as Kapton®, Upilex® and Apical® have a potential for achieving specific power of 1000 W/kg, while the state-of-art specific power of the present day solar cells is 66 W/kg.

This paper describes the preparation of Cu-rich $CuIn_{1-x}Ga_xS_2$ (CIGS2) thin films and solar cells by a process of sulfurization of CuGa-In precursor similar to that being used for preparation of large-compact-grain $CuIn_{1-x}Ga_xSe_2$ thin films and efficient solar cells at FSEC PV Materials Lab. Copper-gallium and indium layers having Cu:(In+Ga) atomic proportion of 1.4:1 were deposited on unheated molybdenum-coated glass substrates by DC magnetron sputtering from CuGa(22%) and In targets. Well-adherent Cu-rich CIGS2 films were obtained by sulfurization in 1-4% hydrogen sulfide diluted in argon at temperatures ranging from 425-500° C for 30-60 minutes. Films tended to peel off when sulfurization was carried out for 60 min at 550° C. Because of indications of excessive indium loss at high (1300 sccm) argon flow rates and low Ar:$H_2S$ (1%) gas proportion during sulfurization, possibly in form of volatile $In_2S$, $H_2S$ gas concentration in argon was increased to 4% and argon flow rate was reduced to 650 sccm. CuGa/In intermixing and sulfur incorporation during sulfurization were promoted by adding intermediate 30 minute steps at 125° C and 325° C so as to avoid indium and gallium globule formation, instead of adding small traces of oxygen. $CuIn_{1-x}Ga_xS_2$ thin films were bluish, dark gray in color. Resistance measurement of CIGS2 films was used to verify if it was Cu-rich or Cu-poor. AES depth profile of unetched Cu-rich CIGS2 thin film showed segregation of excess copper at the surface possibly as a $Cu_{2-x}S$ layer. Excess $Cu_{2-x}S$ near the surface was etched away in dilute (10%) KCN solution for 3 minutes. Atomic proportions of Cu:In:Ga:S of typical Cu-poor CIGS2 films as measured by EMPA at 20 keV incident electron energy was 24.0:19.1:6.9:51.9, corresponding to formula $Cu_{0.92}In_{0.73}Ga_{0.27}Se_2$ thus very near the desired Cu content. A new intermediate chalcopyrite phase $CuIn_{0.7}Ga_{0.3}S_2$ was identified by X-ray diffraction in unetched and etched CIGS2 films. Peaks from a new In-rich phase, probably a new ordered vacancy compound (OVC) $Cu(In_{0.7}Ga_{0.3})_3S_5$, similar to the In-rich OVC phase $CuIn_3Se_5$, were also detected in XRD pattern from etched CIGS2 films. Scanning electron microscopy revealed large (2-2.5 □m) compact-grain morphology for films sulfurized at and above the temperatures of 450° C. Based on visual observations and results of material characterization, sulfurization parameters were optimized as follows: Ar:$H_2S$ of proportion of 1:0.04 and argon flow rate of 650 sccm, 30 minutes each at 125° C and 325° C, and 60 minutes at maximum temperature of 475° C. Four or five, small solar cells were completed by deposition of CdS heterojunction partner layer by chemical-bath deposition, transparent-conducting ZnO/ZnO:Al window bilayer by RF sputtering and vacuum deposition of Ni/Al contact fingers through metal mask on several $CuIn_{1-x}Ga_xS_2$ thin films on Mo-coated 2.5 cmx2.5 cm glass substrates. All the cells showed PV conversion efficiency, □ above 6%, most being over 7% (AM1.5, Total area). PV performance was uniform from one region to another, on the same substrate. AM1.5, total area, PV parameters of the best solar cell were as follows: $V_{oc}$ = 705 mV, $J_{sc}$ = 18.63 mA/cm$^2$, FF = 64.58%, and □ = 8.48%, QE cutoff at 800 nm, equivalent to CIGS2 bandgap of 1.55 eV, showing an actual bandgap increase to the required optimum value for efficient AM0 PV conversion as a result of Ga incorporation.

[1] This work has been supported by the NASA Glenn Research Center at Lewis Field and the National Renewable Energy Laboratory

## 1. INTRODUCTION

Peter Glaser proposed the concept of solar power satellites (SPS) in 1968. In the earlier two studies carried out by NASA and DOE, the concept has been found to be scientifically and technologically feasible. The 1998 Space Solar Power (SSP) Concept Definition Study (CDS) has determined that SSP system performance goals could be accomplished through coordinated, strategic technology development efforts. Because of the estimated launch costs of low earth orbit (LEO) and geosynchronous-earth orbit (GEO) of $ 11,000/kg and $66,000/kg, specific power i.e. power per unit mass becomes very important [1]. 50 μm thick Si cells, without concentration, annealed with $CO_2$ lasers and monocrystalline 5 μm thick gallium arsenide, GaAs, solar cells on synthetic corundum substrates with x2 concentration were considered for SPS. Such a system would require thick single crystal substrates or wafers and interconnections for fabrication of interconnected strings. Integrally interconnected thin-film solar arrays would be free from both the constraints. Significant gains in spacecraft performance can be achieved at lower cost with ultra-lightweight, radiation-resistant, copper-indium sulfide, $CuInS_2$ polycrystalline-thin-film, flexible solar arrays having efficiencies comparable to current silicon solar cell arrays [1,2]. The bandgap of 1.53-1.55 eV of $CuInS_2$ is near the optimum value for an efficient conversion of AM0 solar radiation outside the earth's atmosphere. If necessary, it could also be increased slightly with the addition of small amount of gallium. High solar absorptances of $CuInS_2$ would allow the possibility of fabricating the cells with the absorber layer as thin as 1-2 μm. These cells do not suffer from intrinsic degradation mechanisms as is the case with a-Si:H cells. Copper chalcopyrites $CuIn_{1-x}Ga_x Se_{2-y}S_y$ have the highest radiation tolerances of all known materials. Ultra-light weight thin-film solar cells have a potential for achieving specific power of 1000 W/kg, while the state-of-art specific power of the present day solar cells is 66 W/kg. Higher efficiencies, freedom from intrinsic degradation, and high radiation resistance of $CuInS_2$ thin-film solar cells make them the leading candidate for this purpose.

Currently, copper-indium selenide and cadmium telluride are the leading absorber materials for terrestrial thin-film PV technology [3-10]. Small amounts of gallium and sulfur are added to copper-indium selenide for adjusting the bandgap. The efforts at NASA GRC over the last several years have focused on production of $CuInSe_2$, $CuInS_2$ and related materials through low-temperature methods [11-14]. Polycrystalline-thin-film solar cells of $CuIn_{1-x}Ga_x Se_2$ (CIGS), $CuInS_2$ and CdTe have already shown total-area PV conversion efficiencies of 18.8%, 11.1% (12.5% active area), and 15.8% at air mass 1.5 (AM 1.5) respectively. These are equivalent to conversion efficiencies in the space of ~15.2%, 9.0% and ~12.8% (AM0) respectively. There is considerable potential for enhancing the conversion efficiency of $CuInS_2$ thin-film solar cells. More importantly, thin-film solar cells can be produced economically because of the ease of coating large areas uniformly and reproducibly; and because of the incorporation of steps for monolithically integrated interconnections during the fabrication.

The objective of the present research is to develop ultra-lightweight, radiation-resistant, highly efficient, high specific power $CuIn_{1-x}Ga_xS_2$ (CIGS2) thin-film solar cells for space electric power. Small proportion of gallium is being incorporated so as to obtain benefits of improved adhesion, slightly higher bandgap, and incorporation of back-surface field as has been done with CIGS cells. Initially CIGS2 thin film solar cells are being fabricated on glass substrates. The main thrust is towards development of fundamental understanding and baseline processes rather than attaining the highest efficiencies.

### 1.1 Review of Previous Research

Scheer [15] has reviewed the surface and interface properties of Cu-chalcopyrite semiconductors and devices. A ternary phase diagram of copper-indium-sulfur system shows tie lines between $Cu_2S$ and $In_2S_3$ as well as between InS and CuS pointing to possible pathways for the synthesis of $CuInS_2$. On the indium rich side, it shows the presence of $CuInS_2$ and $CuIn_5S_8$ ternary phases and the binary phase $In_2S_3$. On the copper-rich side, there are only the binary $Cu_{2-x}S$ phases besides the ternary phase $CuInS_2$ [16]. Migge [17] and Migge and Grzanna [18] have estimated free energies of the compounds $In_6S_7$, $In_{2.8}S_4$, $CuInS_2$, $CuIn_5S_8$, and $CuIn_2$ at 298 K and $In_6S_7$, $In_{417}S_{583}$, $In_2S_3$, $Cu_{951}In_{149}$, and $CuIn_5S_8$ at 723 K by thermochemical analysis of Cu-In-S system. The compound $CuInS_2$, is shown to equilibrate with most compounds of the system. Formation of $CuInS_2$ by sulfidization (sulfurization) of Cu-In alloy e.g. $Cu_7In_3$ with $H_2S$ at 723 K by applying a ratio $pH_2S/pH_2 \leq 10^{-5}$ is predicted [18]. More interestingly, even in slightly In-rich film having cation ratio In/Cu+In of ~0.55, both the front and back surfaces are covered by $CuIn_3S_5$ phase showing that In-rich copper-indium sulfide phase segregates at the surfaces of $CuInS_2$ grains [19]. On the other hand, only the front surface shows the presence of copper sulfide even in highly Cu-rich copper-indium sulfide thin films [19]. Thus stoichiometric $CuInS_2$ thin films may be obtained by growing a Cu-rich film and etching away the excess copper sulfide at the surface. This fact has been used in the development of a tolerant two-step process by Klaer et al at the Hahn-Meitner Institute [20]. It consists of sulfurization of sputter deposited copper and indium layers on molybdenum-coated float glass

substrates, in vacuum-evaporated sulfur vapor at 550° C, to form a 2 μm thick copper-rich $CuInS_2$ thin film. Excess $Cu_{2-x}S$ secondary phase acting as a flux can assist in the formation of large grain $CuInS_2$ layer and then can segregate to the surface. It can be removed by etching in a KCN solution leaving behind a slightly copper-poor $CuInS_2$ layer. Solar cells are completed by chemical bath deposition of a thin CdS layer, sputter deposition of ZnO and evaporation of Al contact fingers. The best morphology and PV conversion efficiency of 11.1 % (AM1.5, total area, 12.5% active area) has been obtained at Cu/(Cu+In) ratio of 1.8 [20]. Comparison of $CuInS_2$ thin film growth by co-evaporation, sulfurization, and spray pyrolysis has indicated that CuS segregation at the surface is induced by excess S at the surface and is activated thermally [21]. Earlier, Ogawa et al [22] have prepared 10% (AM1.5) $CuInS_2$ thin-film solar cells by sulfurization of vacuum evaporated copper and indium layers in Argon/$H_2S$ 5% mixture at 550° C.

Gosala et al [23] have found that roughness of coevaporated In-rich Cu-In precursor layers as determined by Rutherford Back Scattering (RBS) can be suppressed by cooling substrates to below room temperature while for Cu-rich precursor films, copper excess must be maintained above 1.4. Sulfurization was carried out in 3 % $H_2S$ at 400° C. 3% solar cells were prepared with $CuInS_2$ thin films prepared from In-rich films deposited on cooled precursors. On the other hand, Cu-excesses over 1.8 led to deterioration of conversion efficiencies probably because KCN etching may not be removing excess copper sulfide completely leading to shunting paths. Miles et al [24] prepared $Cu_{11}In_9$ phase free of inhomogeneous secondary phases by deposition of ~1700 alternate Cu and In layers on Mo-coated glass substrates by magnetron sputtering. Precursor layers were placed face upwards either on strip heaters and excess sulfur was placed underneath at a distance of 10 cm or in a graphite box. Samples were heated after evacuating annealing chambers to 1.3 Pa and sealing. X-ray diffraction (XRD) and optical absorption spectroscopy analyses indicated formation of $CuInS_2$ films, free from binary phases, and with a direct bandgap of 1.45 eV. At annealing temperatures below 300° C, Cu and In binary compounds were detected showing an incomplete reaction. At FSEC PV Materials Lab, sputter-deposited Cu-In precursor layers have been intermixed to form single $Cu_{11}In_9$ phase by modest in-situ heating.

Watanabe et al [25] have sulfidized in Ar/$H_2S$ 5%, stoichiometric and sulfur-deficient Cu-In-S layers sputtered respectively from $Cu_2S$ and $In_2S_3$ mixed powder and $CuInS_x$ powder targets. Better crystallinity and cell properties (1.4%) were observed from $CuInS_2$ thin films prepared by annealing S-deficient amorphous Cu-In-S films. More recently, Watanabe and Matsui [26] deposited Cu-In-S precursors on rotating substrates by reactive sputtering from Cu and In targets in a $H_2S$/Ar mixture. $CuInS_2$ thin films were prepared by annealing in 5% $H_2S$/Ar at 550° C. Randomly oriented needlelike $CuIn_5S_8$ crystallites were observed in $CuInS_2$ thin films formed from precursors containing little S. Large grain, single phase $CuInS_2$ thin films and 6.3% cells were obtained without KCN treatment with Cu-In-S precursors having S/(Cu+In) ratio of 0.3. Grain size and uniformity deteriorated at much higher S/(Cu+In) ratios. Sulfur atoms probably restrain atomic migration thus eliminating indium aggregates on the film surface. However, above the optimum amount, sulfur seems to limit atomic migration excessively reducing grain size and complete intermixing. Ito and coworkers [27] have compared sulfurization of multiple (three) $In_2S_3$/Cu bilayers with that of metallic precursors. Adhesion of $CuInS_2$ thin films was found to improve when a small amount of gallium was deposited prior to the deposition of metallic precursors. Large (5 μm) grain $CuInS_2$ thin films were obtained with the gallium deposition, however, with rough morphology and segregation of islands of $Cu_xS$ and $InS_x$ phases on the surface. Films prepared using multiple $In_2S_3$/Cu bilayers were smooth and more homogeneous. Best typical efficiencies were Cu/In 10.4%, Ga-doped Cu/In 10.4%, $In_2S_3$/Cu 10.6%. Most of the improvement was due to an improvement in the fill factor [27]. Similar to CIGS cells, gallium incorporation has been found to increase the open circuit voltage and efficiencies of $CuInS_2$ cells, even though only small amount of gallium has been detected in the electrically active region near the surface [28]. Recent preliminary results of the growth of Cu-In-Se-S by selenization, sulfurization in $H_2Se$ + $H_2S$ (0.5%) in argon gas mixture at 350° to 450° C showed that a denser $CuInS_2$ films and 8% efficiency can be obtained by first reacting Cu-In layer at 350° C for 30 min followed by a 60 minute reaction at 450° C [29]. Indium segregation was avoided during experiments by adding minute amounts of oxygen ($O_2$/$H_2S$+$H_2Se$=0.01). Yukawa et al [30] have prepared $CuInS_2$ thin films by electrodeposition from an aqueous ternary bath. Well crystallized films were obtained by annealing in vacuum at 673 K without $H_2S$. Hepp and colleagues have prepared GaS, InS and $CuInS_2$ thin films by spray chemical vapor deposition using single-precursor sources [9-12].

Wet chemical oxidation of absorber surface have been found to result in considerable reduction of the reverse saturation current and the diode ideality factor thus improving $CuInS_2$ thin-film solar cell characteristics [31]. Sub-bandgap structure at 1.44 eV has been assigned to donor-acceptor transitions based on temperature dependence of photo- and electroreflectance analysis of CdS/$CuInS_2$ heterostructures [32]. A reasonable correlation has been found to exist between the electron-beam induced current and quantum efficiency of $CuInS_2$ solar cells [33]. Attempts have been made to improve the open circuit voltage of $CuInS_2$ thin-film solar cells by

modifying the grain boundaries and heterointerface by addition of ZnS and CdS [34]. $CuIn_{1-x}Ga_x Se_{2-y}S_y$ thin-film solar cells have been found to possess excellent radiation hardness [35].

Steps for monolithically integrated interconnections can be incorporated during the fabrication of thin-film solar cells. Monolithically integrated, flexible 10% (AM0) $CuInSe_2$ submodule has been fabricated on titanium foil [36]. Solar cell parameters under lunar conditions have been calculated by Dhere and Santiago [37].

CIGS thin-film solar cell technology has evolved considerably over the years [9,10]. On the other hand, considerable work must be performed on $CuInS_2$ thin-film solar cell technology. Especially fundamental understanding must be gained so as to attain the level of maturity comparable to that of CIGS. Because of the similarity between the processes for the synthesis of CIGS and $CuInS_2$ thin films and cell fabrication procedure, much can be learned from the CIGS solar cell technology. CIGS thin films with good crystallinity and smooth morphology having excellent efficiencies have been prepared by initial co-evaporation of indium, gallium and selenium followed by copper and selenium co-evaporation passing through a copper rich film and finishing off with indium, gallium and selenium co-evaporation to obtain an overall Cu-poor film. Contrera et al [38] have fabricated the champion (18.8%) cell by passing through an intermediate Cu-rich phase. However, this does not seem to be as critical for their process at 550° C. In another instance of CIGS thin films deposited by co-evaporation at 550° C, efficiencies of solar cells prepared using an uniform composition all along was higher (15.0%) compared to that (12.9%) prepared using intermediate Cu-excess [29]. However, for deposition at 400° C, uniform composition resulted in a lower (9.5%) efficiency than that (12.9%) obtained with intermediate Cu-excess.

Two-selenization process has been developed at FSEC PV Materials Lab for the deposition of large compact grain $CuIn_{1-x}Ga_xSe_2$ thin films and efficient solar cells [3-8]. It relies on the fluxing action of $Cu_{2-x}Se$ phase in copper-rich CIGS films obtained after the first selenization. Deposition of indium followed by the second selenization converts the entire film into a copper-poor CIGS film suitable for highly efficient solar cells. The excess $Cu_{2-x}Se$ phase is reconverted to CIGS rather than etching it away. Resultant CIGS thin films are considerably more adherent to Mo-coated glass substrates with initial Cu-rich phase [6,7]. A CuGa(22 at. %) alloy target was used to eliminate the problem of sputtering from liquid gallium target. Adhesion improved still further with gallium incorporation. Higher rates of temperature ramp-up to 550°C and a controlled cool-down to 300 °C under continued selenium evaporation helped in enhancing gallium content [5]. Solar cell efficiency of 9.02% was achieved with a $CuIn_{0.82}Ga_{0.18}Se_2$ thin film [4-5]. Addition of gallium and sulfur can raise the band gap of CIGS closer to the optimum value. In post-deposition selenized films, gallium has a tendency to diffuse towards the back contact. Ga incorporation near the back contact provides the back-surface field.

Woodcock et al [39] and Bruton et al [40] have carried out a cost analysis of terrestrial thin-film and c-Si solar cells for annual production level of 500 MW based on the procedure developed by Ugalde et al [41]. A similar study would be beneficial in the planning of manufacturing of space thin-film solar cells.

For space applications it would be necessary to deposit solar cells onto a thin plastic substrates. Thin plastic sheets of polyimides such as Kapton®, (DuPont), Apical® (Allied-Apical), and Upilex® (Ube Industries/ICI America), and uniaxially oriented fluoropolymer teflon are suitable substrates because they are lighter in weight, flexible, shatterproof, durable in UV radiation, and transparent to IR radiation. The polyimides Kapton® and Upilex® can maintain their properties even when heated continuously to temperatures of 270-290° C. Other properties need to be considered when selecting the specific product for coating applications. A square foot of 12.5 μm Upilex sheet weighs only 1.7 g. Polyimide Kapton® has been chosen as the primary material in flexible solar arrays on Space Station Freedom. Fluoropolymer tefzel is stable to 180° C, and is recommended for use as a cover sheet. Plastic cover sheets for radiation protection in space are not available at present. Thin films especially those of noble metals do not adhere well to inert substrates. Usually the sheets are treated with corona discharge to improve adhesion. The corona treatment may not be essential for deposition of films by sputter deposition because of the plasma ambient which provides ion bombardment. An undercoat of chromium, titanium-tungsten, etc have been used to improve the adhesion. Sputter-deposited back molybdenum contact is expected to adhere well to the polymer sheets. Polyimide sheets are readily attacked by atomic oxygen which is the predominant atmospheric species in low earth orbit (LEO). The energy of 3.3-5.5 eV of the atmospheric constituents impinging on the polyimide foils is sufficient to break chemical bonds and allow chemical reaction to occur. Polyimide Kapton sheets have been commercially coated with 650-1300 Å silicon oxide on both sides to minimize the damage by atomic oxygen. The silicon oxide coatings have also been helpful in minimizing the moisture attack. There are indications that handling and processing techniques may increase the number of defects in the coatings. Hence it is necessary to take adequate care during the processing to avoid too many large or continuous defects. Other dielectric coatings could also be used as protective buffer layers.

NASA has developed more transparent polyimide sheets. However, the yellow color of Kapton® will not pose a problem for substrate type $CuInS_2$ thin film solar cells. Times required to reduce the ultimate elongation

of Kapton® from from 70% to 1% by heating in air at 350° C, 400° C and 450° C are for six days, 12 hours and 2 hours respctively. It will last longer in inert ambient and in vacuum. Hence the processing temperatures and times must be minimized for fabrication of flexible ultra-lightweight thin-film solar cells on polyimide substrates.

## 2. EXPERIMENTAL TECHNIQUE

The two-selenization process developed at FSEC PV Materials Lab is being used routinely for preparation of large compact grain $CuIn_{1-x}Ga_xSe_2$ thin films and efficient solar cells. The second selenization is being replaced by sulfurization for the fabrication of $CuIn_{1-x}Ga_x Se_{2-y}S_y$ thin films. Using a similar process, approximately 40% Cu-rich $CuIn_{1-x}Ga_x S_2$ thin films were fabricated by sulfurization of CuGa/In layers on Mo-coated substrates, in $H_2S$/Ar mixtures. The process begins with deposition of ~1 μm thick molybdenum back contact layer on unheated soda-lime float-glass substrates by DC magnetron sputtering in a 47 cm diameter, 60 cm height stainless-steel bell jar pumped with a cryopump and a rotary vacuum pump. Some Mo coated glass substrates were obtained from Siemens Solar Industries. Copper-gallium CuGa(22%) and indium layers were also deposited by DC magnetron sputtering in the same cryopumped vacuum system. Thicknesses of the metallic precursors CuGa(22%) and In calculated so as to obtain an initially 40% cooper-rich CIGS film were as follows: CuGa(22 at.%) 5150 Å and In 3925 Å. The final thickness of the slightly copper-poor $Cu_{0.92}In_{1-x}Ga_xS_2$ layer was projected to be 2.5 μm. Initially the entire thickness (5150 Å) of CuGa(22%) was sputter-deposited on Mo-coated glass substrates followed by deposition of 3925 Å thick In layer. More recently, this has been modified so as to minimize the loss of indium, in the form volatile $In_2S$ during the sulfurization, by covering it with a thin CuGa layer. The new sequence is shown in Figure 1. It consists of the deposition of 70% of CuGa (3605 Å), followed by 100% of In (3925 Å), and finally covered with the remainder 30% of CuGa (1545 Å).

Sulfurization was carried out in flowing argon:$H_2S$ gas mixture. Samples were placed in a 5 cm outer diameter, 45 cm long alumina tube fitted with gas-tight end-caps and glass flow console. Alumina tube was placed in a 5 cm diameter, 30 cm long, single zone furnace. Argon and $H_2S$ flow was measured with gas flow meters. Effluent gas was passed through 2 M KOH aqueous solution in four wash-bottles for scrubbing. For this purpose, two wash bottles were connected in each of two parallel branches to minimize pressure build-up. An initial empty wash bottle prevented inadvertent back-flow of scrubbing fluid. The entire set-up was housed in a fume hood. $H_2S$ gas detector monitored the presence of hydrogen sulfide in the fume hood at parts per million (ppm) level. Care was taken to avoid atmospheric air and moisture contamination by sealing off the gas flow set-up in between experiments. System was primed by passing argon for 120 minutes at a rate of 1300 standard cubic centimeters per minute (sccm) and Ar:$H_2S$ gas mixture for 30 minutes at the preset rate prior to initialization of sulfurization. The flow rate of 1300 sccm is approximately equivalent to the change of entire reaction volume once per minute. Sulfurization temperatures were varied over a range of 425-550° C. Sulfurization time was either 30 or 60 minutes at the maximum temperature. Initially the preset Ar:$H_2S$ gas proportion was maintained at 1:0.01 and the preset argon gas flow rate was 1300 sccm. However, because of indications of excessive indium loss, the preset argon flow rate was reduced to 650 sccm while the preset Ar:$H_2S$ gas proportion was increased to 1:0.04. In earlier selenization experiments, indium has been found to escape in the form of volatile $In_2Se$ at low selenium vapor incidence rates. Argon to hydrogen sulfide gas flows were controlled independently to obtain the desired Ar:$H_2S$ proportion. No oxygen was added to avoid indium and gallium globule formation. Instead, precursor intermixing and sulfur incorporation were promoted by maintaining metallic precursors for 30 minutes each and at 125° C and 325° C under the flow of Ar:$H_2S$ gas mixture at the preset proportion and rate.

Materials properties of CIGS2 thin films were studied for optimizing the preparation parameters. Adhesive strength at the interface of Mo/metallic precursors and Mo\CIGS thin films was tested by a simple adhesive-tape peeling test. Formation of crystalline phases and morphology was studied by X-ray diffraction (XRD) and scanning electron microscopy (SEM). Composition was analyzed by wavelength-dispersive analysis of X-rays i.e. electron probe microanalysis (EMPA) and energy-dispersive analysis of X-rays (EDAX). Composition variation along the depth was analyzed by Auger electron spectroscopy (AES) in conjunction with sputter-etching. Near stoichiometric, slightly Cu-poor CIGS2 thin films were obtained by etching away excess $Cu_{2-x}S$ in 10% aqueous KCN solution for 3 minutes. Solar cells were completed by deposition of ~500 Å CdS heterojunction partner layer by chemical-bath deposition, transparent-conducting ZnO/ZnO:Al window bilayer by RF sputtering and vacuum deposition of Ni/Al contact fingers through metal mask on CIGS2 thin films on Mo-coated glass substrates (Fig. 2). Because of vacuum problems in an existing RF sputtering system, the cells completion and current-voltage IxV and quantum efficiency, QE measurements were carried out at the National Renewable Energy Laboratory (NREL) with the kind help of Dr. Kannan Ramanathan.

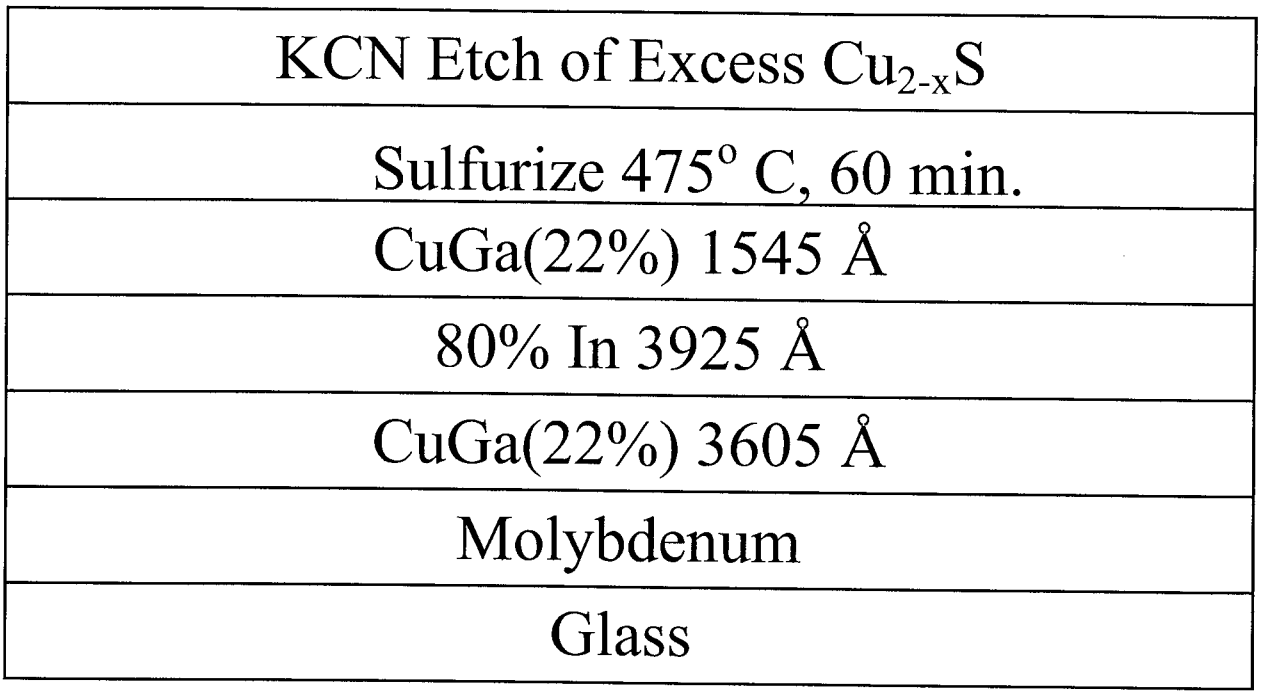


Figure 1. Preparation steps of 2.5 μm thick, nearly stoichiometric, slightly Cu-poor CIGS2 thin film.

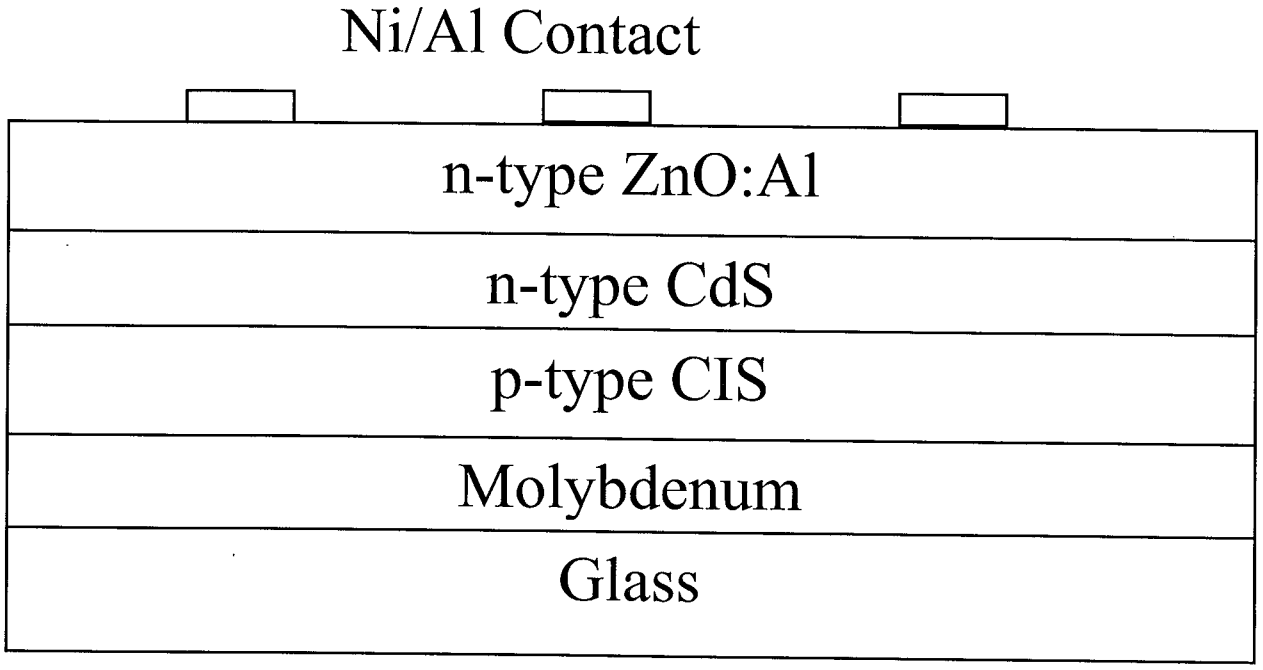


Figure 2. Layer sequence of CIGS2 thin film solar cell.

## 3. RESULTS AND DISCUSSION

Metallic precursors were found to remain on the molybdenum back contact layer, when a transparent adhesive tape was applied onto CuGa/In and CuGa/In/CuGa metallic precursors and peeled off, showing that they adhered well to the molybdenum back contact layer. There was spontaneous, partial peeling off of films after sulfurization for 60 minutes at substrate temperature of 550 °C. Well-adherent films were obtained for sulfurization at maximum temperatures in the range 425-500° C for 60 minutes, in 1-4% $H_2S$ diluted in argon at argon flow rate of 650 sccm.

In case of sulfurization in Ar:$H_2S$(0.5%) mixture at high argon flow rate of 1300 sccm, sides and back of glass substrates and alumina carrier were found to be coated with semitransparent, brownish yellow film, while the CIGS2 film itself was semi-reflecting whitish gray. This indicated excessive indium loss possibly in the form $In_2S$. Earlier indium has been found to escape in the form of volatile $In_2Se$ at low selenium vapor incidence rates. Bluish, dark gray $CuIn_{1-x}Ga_xS_2$ thin films were obtained when the sulfurization were carried out in Ar:$H_2S$(4%) mixture at argon flow rate of 650 sccm.

Composition analysis of Cu-rich and Cu-poor $CuIn_{1-x}Ga_xS_2$ thin films was carried out by EMPA at NREL by Amy Swatzlander Guest. Proportions of atomic concentrations of Cu:In:Ga:S of typical Cu-poor CIGS films was found to be 24.0:19.1:6.9:51.9 at incident electron energy of 20 keV. Thus EPMA composition of Cu-poor CIGS2 thin films seems to correspond to the formula $Cu_{0.92}In_{0.73}Ga_{0.27}Se_2$. This is very near the desired composition in terms of copper content. At incident electron energy of 10 keV, the proportion of gallium as compared to that of indium was lower. This is to be expected because of the lower depth of analytical volume at the lower electron energy and the tendency of gallium to diffuse towards the back contact. In typical Cu-rich CIGS2 films, proportion of atomic concentrations of Cu:In:Ga:S measured at 20 keV was 41.5:9.8:3.8:44.93. At 10 keV, the proportion of copper was still higher. This gives an indication of much higher than desired copper-excess Cu/In+Ga of 1.4-1.8. However, results of EDAX analysis of unetched and etched CIGS2 thin films prepared in the present study were compared with that of unetched and etched reference $CuInS_2$ thin films having copper excess Cu/In+Ga = 1.8 kindly provided by Dr. Roland Scheer at the Hahn-Meitner Institut, Cu-excesses were seen to be comparable.

In a manner similar to the practice with CIGS thin films, a simple resistance measurement test was routinely used to gauge whether the CIGS2 thin film is Cu-rich or Cu-poor. Low resistance (<500 ♦) of the films indicated the formation of copper-rich film whilst a high resistance (>100 k♦) indicated Cu-poor film.

AES analysis of the surfaces of unetched and etched CIGS2 samples showed the presence of S at 152 eV, C at 270 eV, In at 404 eV, O at 510 eV and Cu at 920 eV. Surface of etched CIGS2 sample showed AES peaks of S, C, In, O, Cu and a small Ga peak at 1070 eV. Oxygen and carbon AES peaks disappeared after sputter-etching approximately 500 Å of surface layer with an argon sputter gun. AES depth profile of unetched $CuIn_{1-x}Ga_xS_2$ thin film sample in Figure 3 shows the predominance of a copper-rich phase in an approximately 8500 Å thick surface layer. In this layer, copper excess as measure by ratio Cu/In+Ga of atomic concentration is in the range 4-14. Thus during the sulfurization of copper-rich precursor, the excess copper precipitates at the surface as a $Cu_{2-x}S$ layer. In a similar manner to the case with CIGS thin films, it would provide a fluxing action for improved morphology. Moreover, the remainder of the film is nearly stoichiometric CIGS2. This forms the basis of the process of etching away the excess copper phase in a dilute KCN solution, leaving behind a nearly stoichiometric $CuIn_{1-x}Ga_xS_2$ thin film. The presence of slightly copper-poor, nearly stoichiometric $CuIn_{1-x}Ga_xS_2$ thin film is confirmed by the AES depth profile of an etched CIGS thin film in Figure 4. Concentration increase of gallium towards the back molybdenum contact once again demonstrates the tendency of gallium to diffuse towards the Mo back contact possibly because of the residual stress at that interface. AES depth profiles also explain the increasing gallium concentration and decreasing copper concentration detected in EPMA analysis at higher incident electron energy.

Morphology of CIGS thin films was studied by scanning electron microscopy (SEM). An SEM image of an etched $CuIn_{1-x}Ga_xS_2$ thin film in Figure 5 shows the film to consist of compact, large-grain crystallites. The grain size is estimated at 2-2.5 □m, i.e. comparable to the film thickness.

□-2□ type X-ray diffraction pattern of Cu-rich (unetched) $CuIn_{1-x}Ga_xS_2$ thin film obtained using Cu K☒ X-rays is shown in Figure 6. At present JCPDS data of $CuIn_{1-x}Ga_xS_2$ phase having intermediate compositions between of $CuInS_2$ and $CuGaS_2$ is not available. It was verified that crystallographic parameters 'a' and 'c' of the intermediate chalcopyrite phases: $CuIn_{0.7}Ga_{0.3}Se_2$, $CuIn_{0.6}Ga_{0.4}Se_2$ and $CuIn_{0.5}Ga_{0.5}Se_2$ follow a linear variation between those of $CuInSe_2$ and $CuGaSe_2$. A similar linear extrapolation of 'a' and 'c' parameters between those of $CuInS_2$ and $CuGaS_2$ was employed for indexing the XRD peaks. The values of lattice spacing 'd' of crystallographic planes calculated from 2□ positions of XRD peaks were found to fit crystallographic parameters of

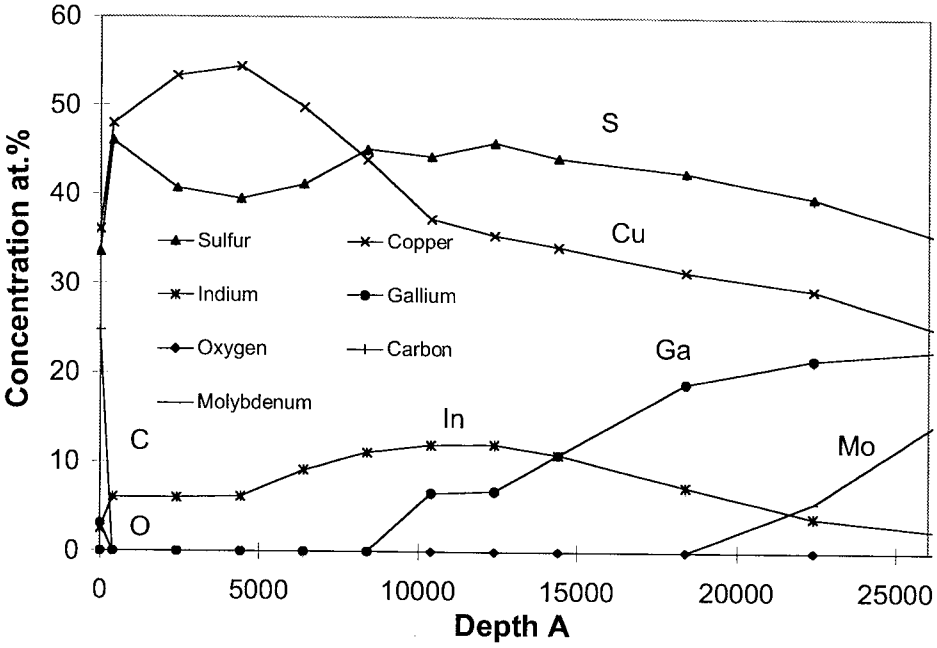


Figure 3. AES depth profile of unetched CIGS2 thin film showing a copper-rich surface layer.

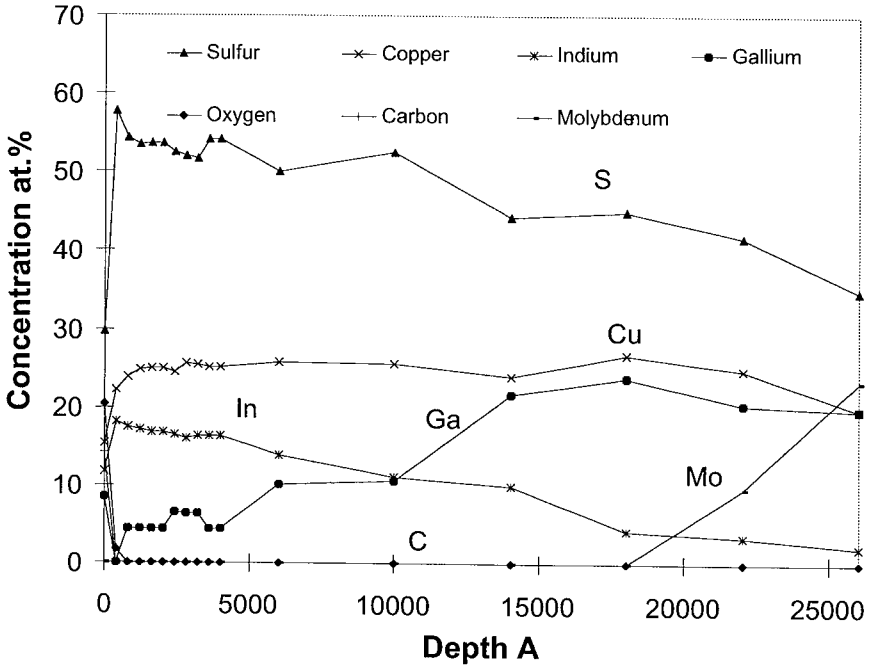


Figure 4. AES depth profile of a near stoichiometric, slightly Cu-poor, etched CIGS2 thin film.

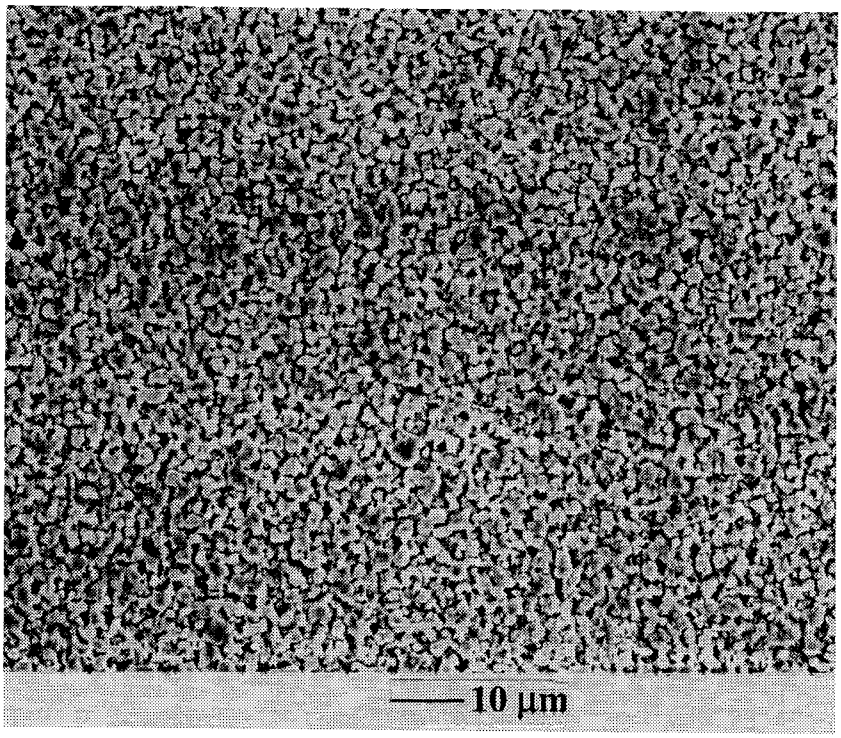


Figure 5. SEM image of a large (2-2.5 µm), compact-grain, etched CIGS2 thin film.

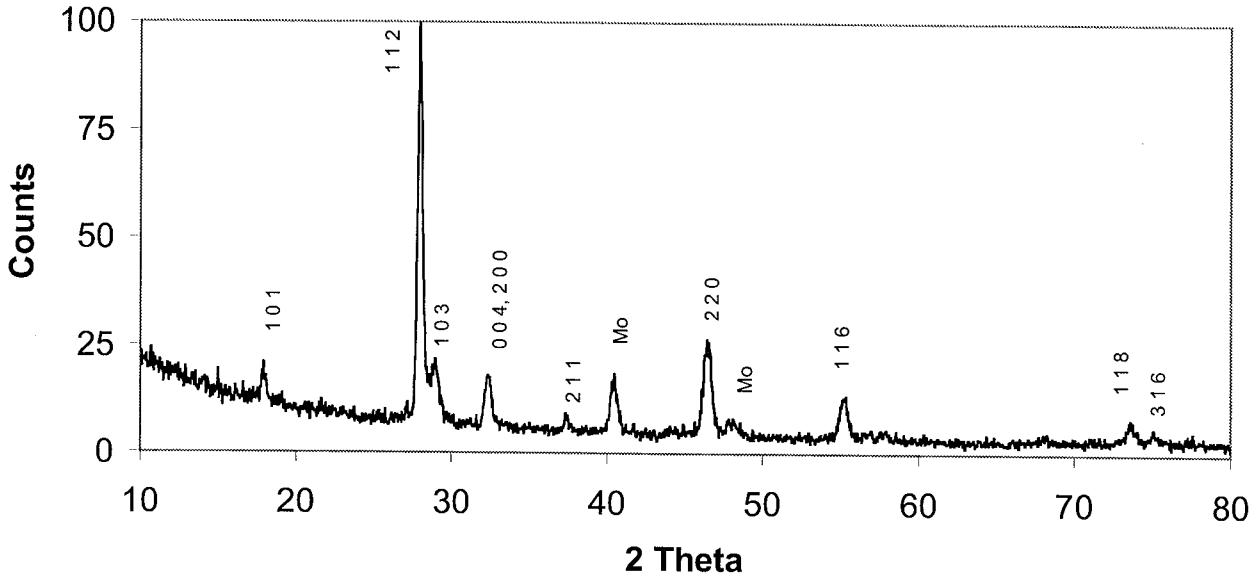


Figure 6. XRD pattern from an unetched, Cu-rich (Cu/In+Ga ≈ 1.4) CIGS2 thin film.

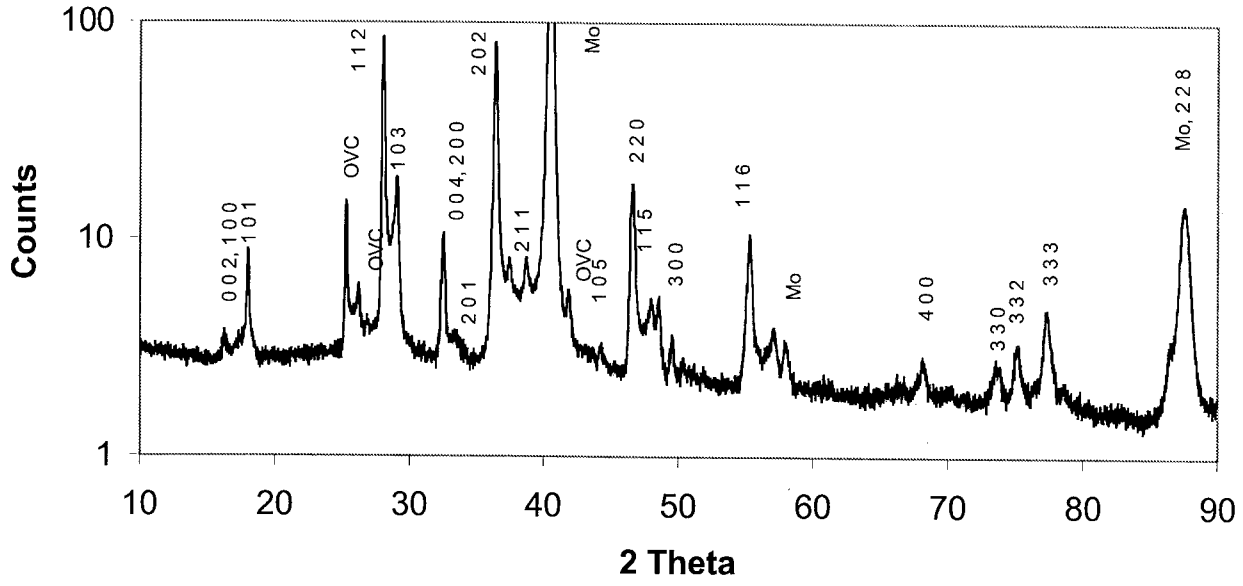


Figure 7. XRD pattern from a near stoichiometric, slightly Cu-poor, etched CIGS2 thin film.

a new chalcopyrite phase $CuIn_{0.7}Ga_{0.3}S_2$ with 'a' = 5.47 Å and 'c' = 10.94 Å. The crystallographic parameters are being refined further. Besides the XRD peaks of molybdenum, the following XRD peaks of the intermediate chalcopyrite phase were identified: 101, 112, 103, 004, 220, 116, and 316. As expected 112 peak is the strongest. X-ray diffraction pattern of Cu-poor (etched) $CuIn_{1-x}Ga_xS_2$ thin film obtained at NREL by Dr. Helio Moutinho is shown in Figure 7. In this case also the calculated lattice spacing 'd' of crystallographic planes again fit well with 'a' and 'c' parameters of the intermediate chalcopyrite phase $CuIn_{0.7}Ga_{0.3}S_2$. XRD peaks of molybdenum were stronger because of the lower thickness of the etched film. The following XRD peaks of the intermediate chalcopyrite phase were identified: 100, 002, 101, 110, 102, 11, 112, 103, 200, 004, 201, 210, 202, 211, 220, 213, 105, 220, 221, 115, 300, 116, 400, 330, 331, 332, 333, 228, and 424. Thus both the XRD patterns unequivocally show the formation of the new intermediate chalcopyrite phase $CuIn_{0.7}Ga_{0.3}S_2$. Three peaks that could not be attributed to either $CuIn_{0.7}Ga_{0.3}S_2$ or molybdenum were again found to arise from an indium-rich intermediate chalcopyrite phase having parameters of 'a' = 6.128 Å and 'c' = 12.257 Å. Possibly it may be a phase $Cu(In_{0.7}Ga_{0.3})_3S_5$. A similar indium-rich phase $CuIn_3Se_5$ has been found to exist at the surface of copper-indium selenide films and has been termed the ordered vacancy (OVC) phase [42]. It is n-type and hence forms a buried homojunction with the p-type CIGS films and is known to lead to high conversion efficiency of solar cells. In the XRD pattern in Figure 7, the following peaks of the chalcopyrite OVC phase $CuIn_{0.7}(Ga_{0.3})_3S_5$ were identified: 112, 103, and 220.

Based on visual observations and results of material characterization, sulfurization parameters were optimized as follows: Ar:$H_2S$ of proportion of 1:0.04 and argon flow rate of 650 sccm, 30 minutes each at 125° C and 325° C, and 60 minutes at maximum temperature of 475° C. Most of the results presented above and in the following pertain to these conditions.

Solar cells were completed at NREL on five substrates. Each possessed an area covered with an etched, near stoichiometric, slightly Cu-poor CIGS2 thin film on Mo-coated glass substrate of 2.5 cm x 2.5 cm. Cell completion began with a deposition of ~500 Å CdS heterojunction partner layer by chemical-bath deposition. Afterwards, a transparent-conducting window bilayer consisting of a thin film of undoped ZnO and a thin film of zinc oxide doped with aluminum was deposited by RF sputtering. Finally Ni/Al contact fingers were deposited by vacuum evaporation through metal mask (Fig. 2). Three to five small cells were scribed on each substrates to

test for uniformity. Current versus voltage (IxV) characteristics were measured under simulated AM1.5 conditions at 25° C. All the devices showed photovoltaic activity with the minimum efficiency, □ of 6%, most having efficiency >7% (AM1.5, Total area). On the same substrate, the performance was uniform from one region to another. Open circuit voltage, $V_{oc}$ ranged between 650-728 mV. Short circuit current density, $J_{sc}$ was in the range 16.8-19.2 mA/cm$^2$ and the fill factor, FF ranged between 50-65%. The fill factor seemed to be limited by high series resistance. The devices are undergoing heat treatment at 200° C in air and are expected to improve. So far, PV parameters of the best cell were as follows: $V_{oc}$ = 705 mV, $J_{sc}$ = 18.63 mA/cm$^2$, FF = 64.58%, and □ = 8.48% (Figure 8). Quantum efficiency, QE measurement showed a maximum of 83% absolute external efficiency, with a reasonably flat response over the 550-730 nm range, and high wavelength i.e. absorber bandgap cutoff at 800 nm equivalent to CIGS2 bandgap of 1.55 eV. It is interesting to note that high wavelength cutoff of $CuInS_2$ thin films prepared with 80% Cu-excess at Hahn-Meitner Institut is ~825 nm equivalent to CIGS2 bandgap of 1.50 eV. Thus it can be seen that gallium incorporation has in fact increased the bandgap to the required optimum value for efficient AM0 PV conversion. After further photovoltaic characterization at NREL by IxV and under AM1.5 conditions, the solar cells will be brought to NASA Glenn Research Center for performance evaluation under AM0 conditions.

## 4. CONCLUSIONS

Well-adherent, nearly stoichiometric, slightly copper-poor, large (2-2.5 □m) compact grain, CIGS2 thin films approximately corresponding to formula $Cu_{0.92}In_{0.73}Ga_{0.27}Se_2$ were prepared on Mo-coated glass substrates by sulfurization of a 40% Cu-rich sputter-deposited stack of CuGa(22%)/In/CuGa(22%) metallic precursors in 4% $H_2S$ diluted in argon, at argon flow rate of 650 sccm and maximum temperature of 475° C for 60 minutes, with intermediate 30 minute steps at 125° and 325° C, after etching away excess $Cu_{2-x}S$ near the surface in dilute (10%) KCN solution for 3 minutes. A new intermediate chalcopyrite phase $CuIn_{0.7}Ga_{0.3}S_2$ was identified by XRD in unetched and etched CIGS2 films. Peaks from a new In-rich phase, probably a new ordered vacancy compound $Cu(In_{0.7}Ga_{0.3})_3S_5$, were also detected in XRD pattern from etched CIGS2 films. Several $CuIn_{1-x}Ga_xS_2$ thin film solar cells with PV conversion efficiency exceeding 7% (AM1.5, Total area) were fabricated. The best AM1.5, total area, PV parameters were $V_{oc}$ = 705 mV, $J_{sc}$ = 18.63 mA/cm$^2$, FF = 64.58%, and □ = 8.48%, and QE cutoff at 800 nm, equivalent to CIGS2 bandgap of 1.55 eV, showing an actual bandgap increase to the required optimum value for efficient AM0 PV conversion as a result of Ga incorporation.

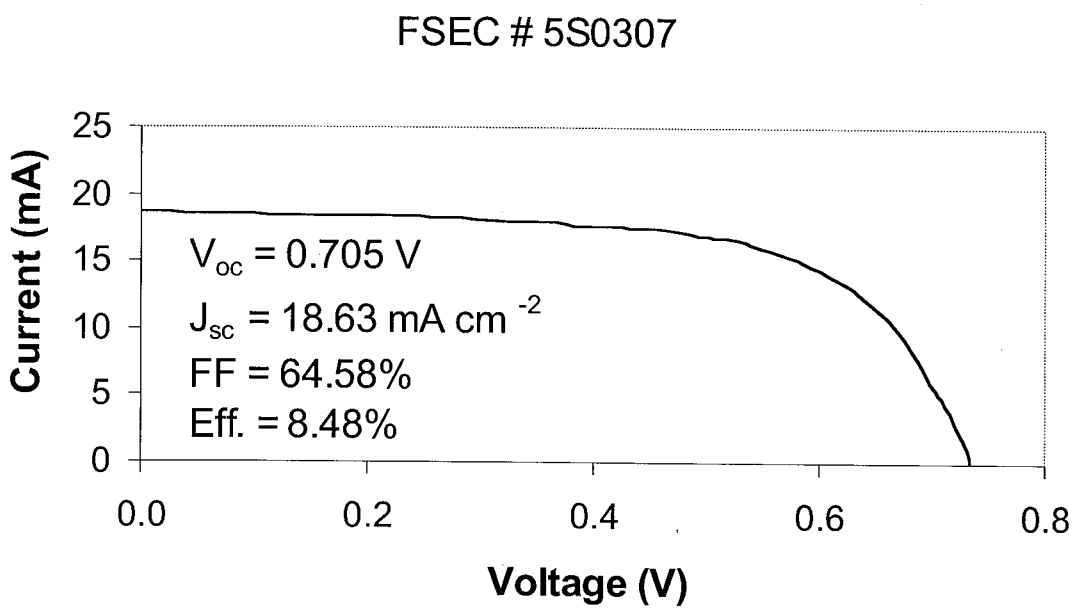


Figure 8. IxV characteristics of CIGS2 thin film solar cells under AM1.5 conditions.

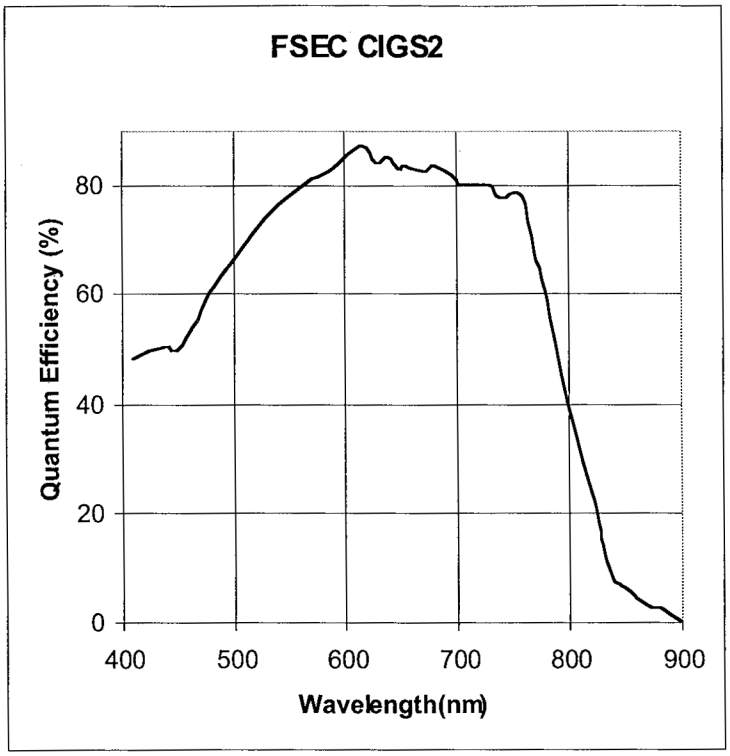


Figure 9. External quantum efficiency of CIGS2 thin film solar cells.

## 5. REFERENCES


1. S. G. Bailey and D. J. Flood, Prog. Photovolt. Res. Appl. **6**, (1998), 1-14.
2. D. J. Flood, Prog. Photovolt. Res. Appl. **6**, (1998), 187-192.
3. N. G. Dhere and K. W. Lynn, Proc. 2nd World Conf. Exhibit. Photovoltaic Solar Energy Conv. (WCEPVSEC), Vienna, (1998), 1125-1128.
4. N. G. Dhere and K. W. Lynn, Proc. 25th Photovoltaic Specialists' Conf. (PVSC), Washington, (1996), 897-900.
5. N. G. Dhere and K. W. Lynn, Solar Energy Mat. & Solar Cells, **41/42**, (1996), 271-279.
6. N. G. Dhere, S. Kuttath, and H. R. Moutinho, J. Vac. Sci. Technol. **A13**, (1995), 1078-1082.
7. N. G. Dhere, S. Kuttath, K. W. Lynn, R. W. Birkmire, and W. N. Shafarman, Proc. 1st WCEPVSEC, Hawaii, (1994), 190-193.
8. N. G. Dhere, D. L. Waterhouse, K. B. Sundaram, O. Melendez, N. R. Parikh, B. K. Patnaik, J. Mat. Sci.: Mat. in Electronics, **6**, (1995),52-59.
9. H. S. Ullal, K. Zweibel and B. von Roedern, 26th PVSC, Anaheim, CA, (1997), 301-305.
10. K. Ramanathan, R. N. Bhattacharya, J. Granata, J. Webb, D. Niles, M. Contreras, H. Wiesner, F. S. Hasoon and R. Noufi, 26th PVSC, Anaheim, CA, (1997), 319-322.
11. A.F. Hepp, M.T. Andras, S.G. Bailey, and S.A Duraj, Adv. Mater. for Optics and Elec. **1**, (1992), 99-103.
12. R.P. Raffaelle, H. Forsell, T. Potdevin, R. Friedfeld, J.G. Mantovani, S.G. Bailey, S.M. Hubbard, E.M. Gordon, and A.F. Hepp, Solar Energy Materials & Solar Cells, **57**, (1999), 167-178.
13. J.A. Hollingsworth, W.E. Buhro, and A.F. Hepp, Chemical Vapor Deposition **5**, (1999), 000-000.
14. J.A. Hollingsworth, W.E. Buhro, A.F. Hepp, D.O. Henderson, A. Ueda, P.P. Jenkins, and M.A. Stan, Solid State Electronics **43**, (1999), 000-000
15. R. Scheer, Trends in Vac. Sci. & Technol. **2**, (1997), 77-112.
16. Chr. Dzionk, M. Brüssler and H. Metzner, Nuclear Instr. & Methods in Phys. Res. **B63**, (1992), 231-235.

17. H. Migge, J. Mater. Res., **6**, (1991), 2381-2386.
18. H. Migge and J. Grzanna, J. Materials Res., **9**, (1994), 125-131.
19. R. Scheer and H. -J. Lewerenz, J. Vac. Sci. Technol. **A13**, (1995), 1924-1929.
20. J. Klaer, J. Bruns, R. Henninger, K. TIIpper, R. Klenk, K. Ellmer and D. Br&unig, 2nd WCEPVSEC, Vienna, (1998), 537-540.
21. R. Scheer, I. Luck, S. Hessler, H. Sehnert, and H. J. Lewerenz, 1st WCEPVSEC, Hawaii, (1994), 160- 163.
22. Y. Ogawa, S. Uenishi, K. Tohyama, and K. Ito, Solar Energy Mat. Solar Cells, **35**, (1994), 157.
23. M. Gossla, H. Metzner and H. -E. Mahnke, 2nd WCEPVSEC, Vienna, (1998), 593-596.
24. R. W. Miles, K. T. R. Reddy and I. Forbes, 2nd WCEPVSEC, Vienna, (1998), 496-499.
25. T. Watanabe, M. Matsui and K. Mori, Solar Energy Materials and Solar Cells, **35**, (1994), 239-245.
26. T. Watanabe and M. Matsui, Jpn. J. Appl. Phys., **35**, (1996), 1681-1684.
27. Y. Hashimoto, T. Ohashi, K. Shimoyama, K. Ichino and K. Ito, 2nd WCEPVSEC, Vienna, (1998), 589-592.
28. I. Hengel, R. Klenk, E. Garc☼a Villora and M. -Ch. Lux-Steiner, 2nd WCEPVSEC, Vienna, (1998), 545-548.
29. R. Birkmire and M. Engelmann, AIP Proc. NCPV Photovoltaics Program Review, (1998), 23-28.
30. T. Yukawa, K. Kuwabara and K. Koumoto, Thin Solid Films, **286**, (1996), 151-153.
31. M. Weber, R. Scheer and H. J. Lewerenz, 2nd WCEPVSEC, Vienna, (1998), 565-568.
32. R. Henninger, K. TIIpper, J. Bruns, J. Klaer and D. Br&unig, 2nd WCEPVSEC, Vienna, (1998), 561-564.
33. R. Scheer, M. Wilhelm, V. Nadenau, H. W. Schock and L. Stolt, 14th European PV Solar Energy Conf. (EPVSEC), Barcelona, (1997), 1299-1302.
34. D. Braunger, Th. D≈rr, D. Hariskos, Ch. KIIble, Th. Walter, N. Wieser and H. W. Schock, 25th PVSC, Washington, (1996), 1001-1004.
35. K. Weinert, G. Lippold, M. V. Yakushev, R. D. Tomlinson, R. Klenk and V. Nadenau, 2nd WCEPVSEC, Vienna, (1998), 3679-3682.
36. B. Basol and V. J. Kapur, 13th Space PV Res. Technol. (SPRAT) Conf., (1994), 101-106.
37. N. G. Dhere and J. V. Santiago, Proc. 12th Space Photovoltaic Research and Technology Conference (SPRAT XII), (1992), p. 298.
38. M. Contreras, B. Egaas, K. Ramanathan, J. Hiltner, F. Hasoon and R. Noufi, Progress in Photovoltaics, **7**, (1999), 311-316.
39. J. M. Woodcock, H. Schade, H. Maurus, B. Dimmler, J. Springer and A. Ricaud, 14th EPVSEC, Barcelona, (1997), 857-860.
40. T. M. Bruton, G. Luthardt, K-D Rasch, K. Roy, I. A. Dorrity, B. Garrard, L. Teale, J. Alonso, U. Ugalde, K. De Clerq, J. Nijs, J. Szlufcik, A. Rauber, W. Wettling and A. Vallera, 14th EPVSEC, Barcelona, (1997), 11-16.
41. Ugalde, J. Alonso, T. M. Bruton, J. M. Woodcock, K. Roy, and K. De Clerq, 14th EPVSEC, Barcelona, (1997), 897-900.
42. M. A. Contreras, H. Wiesner, R. Matson, J. Tuttle, K. Ramanathan, and R. Noufi, Mat. Res. Soc. Proc., **426**, (1996), 243-254.